Plant Molecular Biology (2005) 58:669–685
DOI 10.1007/s11103-005-7702-x

Pattern formation in the monocot embryo as revealed by *NAM* and *CUC3* orthologues from *Zea mays* L.

Roman Zimmermann and Wolfgang Werr*
*Institut für Entwicklungsbiologie, Gyrhofstr. 17, D-50923, Köln, Germany (*author for correspondence; e-mail werr@uni-koeln.de)*

Received 17 December 2004; accepted in revised form 21 May 2005

Key words: coleorhiza, maize embryogenesis, *NAM/CUC*, root cap, shoot apical meristem

Abstract

All aerial parts of a higher plant originate from the shoot apical meristem (SAM), which is initiated during embryogenesis as a part of the basic body plan. In contrast to dicot species, the SAM in *Zea mays* is not established at an apico-central, but at a lateral position of the transition stage embryo. Genetic and molecular studies in dicots have revealed that members of the *NAC* gene family of plant-specific transcription factors such as *NO APICAL MERISTEM* (*NAM*) from *Petunia* or the *CUP-SHAPED COTYLEDON* (*CUC*) genes from *Arabidopsis* contribute essential functions to the establishment of the SAM and cotyledon separation. As an approach to the understanding of meristem formation in a monocot species, members of the maize *NAC* family highly related to the *NAM/CUC* genes were isolated and characterized. Our phylogenetic analysis indicates that two distinct *NAM* and *CUC3* precursors already existed prior to the separation of mono- and dicot species. The allocation of the two maize paralogues, *ZmNAM1* and *ZmNAM2* together with *PhNAM*, *AtCUC2* and *AmCUP* in one sub-branch and the corresponding expression patterns support their contribution to SAM establishment. In contrast, the *ZmCUC3* orthologue is associated with boundary specification at the SAM periphery, where it visualizes which fraction of cells in the SAM is committed to a new leaf primordium. Other maize *NAC* gene family members are clearly positioned outside of this *NAM/CUC3* branch and also exhibit highly cell type-specific expression patterns.

Introduction

During embryogenesis, plant cells acquire distinct developmental fates through the coordinated action of pattern formation processes (Jurgens, 1992). As a result, a multicellular embryo with a simple body plan is established. The dicotyledonous embryo is oriented along an apical–basal axis and consists of the shoot apical meristem (SAM) located between two cotyledons, a hypocotyl, the primary root and the root meristem. In contrast, monocotyledonous species such as *Zea mays* develop embryos with a more complex architecture: here, the embryonic axis is displaced laterally relative to the scutellum, which is widely considered to be the single maize cotyledon (Roth, 1955). The SAM is established at a lateral position at the adaxial side of the transition stage embryo opposite to the scutellum. The shoot and root apical meristems at distal ends of the embryonic axis are protected by the coleoptile and coleorhiza, two organs exclusively found in grass species (Tillich, 1977). Histologically, the SAM also differs in structure and function among higher plants: in dicots, it is organized into three distinct clonal layers (Sussex, 1989; Jurgens, 1992; Kerstetter and

Hake, 1997) but it is unclear whether monocot species such as *Zea mays* develop a distinct L2-layer (Abbe *et al*., 1951; Steffensen, 1968). In contrast to dicots such as *Arabidopsis*, the maize SAM acquires activity earlier during embryogenesis itself and forms 6 true leaves prior to seed dormancy. The maize embryo therefore already represents an elaborated miniature plantlet within the maize kernel. All aboveground organs of a plant originate from the SAM, which maintains a stable population of pluripotent stem cells as the source for the generation of new organs (Waites and Simon, 2000). In monocots and dicots, the development of aerial plant organs therefore depends on the establishment of a functional SAM during embryogenesis.

Most of our knowledge about the molecular mechanisms underlying SAM formation in higher plants is derived from work in dicotyledonous species, where members of the *NAC* gene family have been shown to be crucial for SAM initiation. Seedlings mutant for the *Petunia hybrida* gene *NO APICAL MERISTEM* (*PhNAM*) lack a functional SAM and this is accompanied by the fusion of cotyledons along their margins (Souer *et al*., 1996). In *Antirrhinum majus*, mutations in the recently identified *CUPULIFORMIS (AmCUP)* gene cause a similar phenotype although dramatic organ fusions occur throughout development (Weir *et al*., 2004). In *Arabidopsis*, only double or triple mutant combinations of the *CUP-SHAPED COTYLEDON* genes (*AtCUC1-3*) result in loss of the SAM anlage and cotyledon-fusion, suggesting a higher degree of redundancy in the *Arabidopsis* genome (Aida *et al*., 1997; Vroemen *et al*., 2003). One of the key determinants of SAM function in *Arabidopsis* is the homeobox gene *SHOOT MERISTEMLESS* (*STM*), generally considered to confer meristem identity on a cellular level. *AtCUC1* and *AtCUC2* act upstream of *STM*, and the lack of *STM* expression in *cuc1cuc2* double mutant embryos may account for the shoot meristemless phenotype (Aida *et al*., 1997, 1999). In *Arabidopsis* embryos, the initial stripe of *AtCUC2* expression prepatterns the boundary between both prospective cotyledons, which is reflected in a stripe-shaped *STM* pattern. During later stages, the *AtCUC2* and *STM* transcription patterns show complementarity with *AtCUC2* transcripts being excluded from the SAM and confined to two small regions between cotyledon margins (Long and Barton, 1998; Aida *et al*., 1999). *AtCUC1* and *AtCUC3* are expressed in a similar way although *AtCUC3* expression in general is associated with a broader spectrum of boundaries including the base of lateral roots and trichomes. According to available genetic data and expression patterns, *AtCUC3* consistently encodes a major determinant of boundary specification, whereas *AtCUC2* is most essential for SAM initiation (Vroemen *et al*., 2003). Recently, both *AtCUC1*- and *AtCUC2* genes have shown to be controlled post-transcriptionally by *miR164* (Laufs *et al*., 2004; Mallory *et al*., 2004a). Highly conserved miRNA target sites are also present in *AmCUP* and *PhNAM* but not in *AtCUC3* (Mallory *et al*., 2004a) suggesting that expression of the redundant *AtCUC* genes may be controlled differently.

The *NAC* family was named according to its founding members *NAM*, *ATAF1/2* and *CUC2* but has since grown to form a major family in plant species without corresponding counterparts in the animal kingdom. According to genome annotations, 105 *NAC* genes are present in *Arabidopsis* (Duval *et al*., 2002), whereas the rice genome contains 75 *NAC* genes (Ooka *et al*., 2003). Apart from SAM initiation and organ separation, *NAC* family genes have been shown to contribute to various aspects of plant development including flower development (Sablowski and Meyerowitz, 1998), lateral root formation (Xie *et al*., 2000) or hormone response (Ernst *et al*., 2004). Characteristic for every member is the presence of a highly conserved *NAC* domain at the amino-terminus, which can be divided into five discrete subdomains (Kikuchi *et al*., 2000). The *NAC* domain has been shown to bind DNA (Duval *et al*., 2002), and results from X-ray crystallography suggest that it represents a novel transcription factor motif consisting of a twisted beta-sheet surrounded by several helical elements (Ernst *et al*., 2004).

According to molecular and genetic data, the *NAC* gene family contains several attractive candidate genes with which to approach essential aspects of plant development on an evolutionary scale. To study SAM formation in monocot embryos and to compare it to dicotyledonous species, we screened for close relatives of *PhNAM* or *AtCUC1-3* in *Zea mays*. Here, we describe the isolation of the maize orthologues *ZmNAM1*,

ZmNAM2 and *ZmCUC3* based on the phylogeny of the highly conserved *NAC* domain. On the cellular level, the expression patterns of these genes provide insights into pattern formation processes in the maize embryo such as SAM establishment and function. The comparison to *Arabidopsis* not only reveals substantial conservation of patterns but also highlights fundamental differences during early embryo development. During the vegetative phase, a precise boundary between the SAM and the base of the leaf primordium indicates that a large fraction of cells, representing approximately 1/3 of the sectioned area, is recruited into the new primordium (P1) at the flank of the apex.

Material and methods

Cloning of NAC genes from Zea mays

Maize NAC domain amplicons were obtained using degenerate primers 5′-GAR-AAR-GAR-TGG-TAY-TTY-TT-3′ and 5′-TAY-TCR-TGC-ATN-AYC-CAR-TT-3′ in RT-PCR experiments with cDNA derived from embryonic mRNA as the template. Those three fragments encoding the highest homology to the corresponding region in *PhNAM* and *AtCUC1/2*, respectively were combined into one probe to screen a leaf-stage 1 embryo cDNA library cloned into Zap II (Stratagene, kindly provided by Dr. Peter Rogowsky, Lyon). Full-length cDNA clones of *ZmNAC4-6* were isolated and excised *in vivo* by use of the ExAssist Helper Phage® (Stratagene) and subjected to sequence analysis.

The *ZmCUC3*, *ZmNAM1* and *ZmNAM2* full-length cDNA sequences were isolated by 3′ RACE based on genomic or EST sequence data available from www.plantgdb.org (accession numbers see below). For 3′ RACE, total RNA was extracted using TRIzol® (Invitrogen) according to the manufacturer's protocol. One μg of total RNA was treated with DNAseI (Promega) and first strand cDNA synthesis was carried out according to the manufacturer's instructions using SuperScriptII™ reverse transcriptase (Invitrogen) in combination with the 3′ RACE start primer 5′-CCA-CGA-GTC-GAC-TCT-AGA-GCT-CGG-ATC-CTT-TTT-TTT-3′. Resultant cDNA was treated with RNaseH (GIBCO BRL) to remove residual RNA, and the concentration of all samples was adjusted to 50 ng/μl. The 3′ RACE reverse primers were 3′RACER1 (5′-CCA-CGA-GTC-GAC-TCT-AG-3′) and 3′RACER2 (5′-CTC-TAG-AGC-TCG-GAT-CC-3′). In the case of *ZmCUC3*, forward primers were: BQ778932F1 (5′-TGA-GAG-TGC-AGA-TTG-GCA-AGG-3′) and BQ778932F2 (5′-CTT-TCC-CCT-CTT-GGA-TTC-TCC-3′). Forward primers for *ZmNAM1* were BZ782732F1 (5′-GAG-GGT-GTT-CCA-GAA-GCC-AG-3′) and BZ782732F2 (5′-AGT-CCT-GCT-TCT-CGG-ACT-CC-3′). The *ZmNAM1*-directed PCR resulted in two independent amplicons. *ZmNAM2* covers the partially overlapping sequences BZ536377 and BZ782732, whereas the *ZmNAM1* coding sequence is included in accession ZmGS-Stuc04-27-04.6311. Primer pairs for *ZmCUC3* and *ZmNAM1* RT-PCR analyses were BQ778932F1 and BQ778932R1 (5′-GAG-CGT-CTT-CTT-CAT-GCC-GAG-G-3′) and *ZmNAM1*F1 (5′-CTC-ACC-GTC-ACG-GAC-ACT-TCC-3′) and *ZmNAM1*R1 (5′-AGC-CAC-ATC-CTG-ATA-CTA-ATC-3′), respectively.

Computational and database analysis

Analysis of DNA and protein sequences was performed using the Wisconsin GCG software package version 7.0 (University of Wisconsin Genetics Computer Group). Homology searches were performed using tblastn with default parameters at either NCBI (http://www.ncbi.nlm.nih.gov/blast/), DDBJ (http://www.ddbj.nig.ac.jp/) or the Plant Genome Database (http://www.plantgdb.org). Multiple sequence alignments were performed using ClustalW (http://www.ebi.ac.uk/clustalw/) and BOXSHADE (http://searchlauncher.bcm.tmc.edu /multi-align/multi-align.html). Phylogenetic and molecular evolutionary analyses were based on the Neighbour-Joining (NJ) and Maximal Parsimony (MP) methods using MEGA version 2.1 (Kumar *et al.*, 2001). Sequences selected for the phylogenetic tree presented in Figure 1 are as follows: *AmCUP*, AJ568269; *AtCUC1-3*, BAB20598/BAA19529/AAP82630; *AtNAC1*, AAF21437; *AtNAP*, O49255; *OsCUC3*, AP006049; *OsNAC7*: BAA89801; *OsNAM*: AP003542; *PhNAM*: CAA63101; *TaGRAB1*: CAA09371; *TaGRAB2*: CAA09372; *ZmCUC3*: AJ833968; *ZmNAM1*: AJ833966; *ZmNAM2*: AJ833967; *ZmNAC4*: AJ833963;

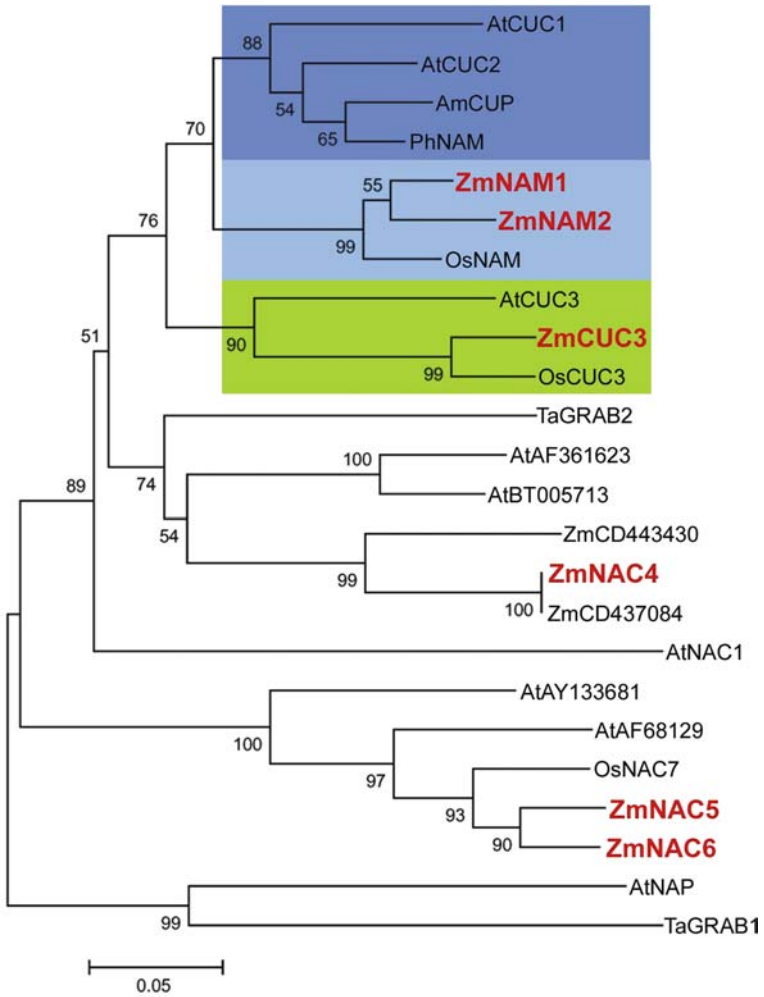

Figure 1. Phylogenetic relationships for *PhNAM*/*AtCUC* relatives inferred from the conserved NAC domain. The dicot group of the NAM sub-branch is highlighted in dark-blue, the monocot group in light-blue. The CUC3 sub-branch is shown in green. The corresponding accession numbers are listed in the materials and methods section. At = *Arabidopsis thaliana*, Am = *Antirrhinum majus*, Os = *Oryza sativa*,, Ta = *Triticum aestivum*, Zm = *Zea mays*.

ZmNAC5: AJ833964; *ZmNAC6*: AJ833965; AtAF361623; AtAF68129; AtAY133681; AtBT005713; ZmCD437084; ZmCD443430.

In situ *hybridization*

For non-radioactive *in situ* hybridization, samples were dissected and fixed at 4 °C overnight in 4% formaldehyde in phosphate-buffered saline, dehydrated in an ethanol series and embedded in paraffin wax (Paraplast® plus, SIGMA). For sections of maize embryos, kernels were trimmed on both sides parallel to the embryo axis for better penetration of the formaldehyde fixative and the wax solution. Paraffin wax-embedded tissue was sectioned by use of a Leica RM 2145 rotary microtome and mounted on coated slides (Super-Frost®Plus). Probes for *in situ* hybridization were cloned either in sense or anti-sense orientation to the T7 promotor and then used as a template for synthesis of digoxigenin-labelled RNA probes using T7 RNA polymerase as described by Bradley *et al*. (1993). RNA *in situ* hybridization was performed according to the method of Jackson *et al*. (1991). *In situ* probes for maize *NAC* genes were chosen to correspond to the C-terminal parts and 3′UTR: *ZmCUC3*, position 483-1143 of accession AJ833968; *ZmNAM1*, position 580-1241 of

accession AJ833966; *ZmNAM2*, position 643-1315 of accession AJ833967; *ZmNAC4*, position 554-1255 of accession AJ833963; *ZmNAC5*, position 489–1372 of accession AJ833964; *ZmNAC6*, position 482–1263 of accession AJ833965. The probe for *kn1* corresponded to the mRNA sequence of accession AY312169, the probe used to detect *ZmSCR* transcripts corresponded to position 2477–3058 of accession AF263457.

Light microscopy and image processing

Nomarsky images were taken using an *Axioskop* microscope in combination with an *Axiocam* camera (*Zeiss*, Germany). Pictures were digitalized using *Axio Vision* software version 3.06 and processed with Adobe® Photoshop® version 7.0.

Results

Molecular cloning and mapping of NAM/CUC *relatives from Zea mays*

Two alternative experimental strategies were pursued to isolate maize relatives of the *NAM* or *CUC* genes from *Petunia* or *Arabidopsis*, respectively (Souer *et al*., 1996; Aida *et al*., 1997; Vroemen *et al*., 2003). The use of degenerate primers for highly conserved amino acid motifs within the *NAC* domain led to the amplification of eight different *NAC* domain fragments from genomic DNA or embryonic cDNA. Three amplicons most related to *PhNAM*/*AtCUC* were combined to screen a leaf-stage I cDNA library. The isolation of corresponding full-length cDNA clones confirmed expression of the *ZmNAC4*, *ZmNAC5*, *ZmNAC6* genes shortly after the SAM first becomes active in the maize embryo. A parallel approach, using maize sequence information available in public databases, led to the identification of three additional maize genes. Initially partial sequence information contained in entries BQ778932 and BZ536377 (www.plantgdb.org) and 3′RACE on embryonic cDNA led to isolation of *ZmNAM1* and *ZmNAM2* (= BZ536377) and *ZmCUC3* (= BQ778932). In total therefore, six maize *NAC* genes closely related to *PhNAM*/*AtCUC* were isolated and subjected to a detailed phylogenetic and embryonic pattern analysis.

The chromosomal map positions of five maize genes are summarized in Table 1. Allocation of *ZmNAC4* to a maize chromosome was not performed since its expression pattern is endosperm-specific (see below). The map positions suggest that *ZmNAM1* (acc. no. AJ833966) and *ZmNAM2* (acc. no. AJ833967) as well as *ZmNAC5* (acc. no. AJ833964) and *ZmNAC6* (acc. no. AJ833965) may be considered paralogues, since the corresponding regions on chromosome 6 are found duplicated on chromosome 3 or 9, respectively. However, the marker saturation is low around the centromere, which slightly obscures this conclusion. Except for *ad**-*N613B* (adherent leaf), which maps close to *ZmCUC3* on chromosome 1, no known developmental mutation is located proximal to the residual gene positions. The EMS-induced mutation *ad**-*N613B* exhibits tightly rolled first leaves which are fused along the midrib. However, sequencing of the *ZmCUC3* coding region and RT-PCR analyses in homozygous mutant plants (data not shown) did not reveal a mutation in the *ZmCUC3* gene, although subtle changes in pattern and timing of *ZmCUC3* gene expression in the *ad**-*N613B* mutant can not be excluded.

Phylogeny of maize NAM/CUC *relatives*

A detailed phylogenetic analysis on available sequences in public databases based on the protein sequence of the NAC domain resulted in a dendrogram partially depicted in Figure 1. Use of the NJ method gave a similar tree to that using the maximum-parsimony algorithm. According to both methods (Kumar *et al*., 2001), the six maize NAC domain proteins group into three discrete branches.

Table 1. Chromosomal map positions of five *NAC* genes with corresponding coordinates and flanking markers.

	ZmNAC5	*ZmNAC6*	*ZmCUC3*	*ZmNAM1*	*ZmNAM2*
Chromosome	6L	9	1	6	3
Coordinate	6.04	9.03	1.06	6.00–6.01	3.05
Flanking markers	*umc1857*/*umc2006*	*umc1258*/*umc1271*	*asg58*/*ntf1*	*umc85a*/*bnlg1867*	*umc102*/*umc1102*

Proteins in the NAM/CUC branch constitute two distinct sub-branches: a CUC3-related sub-branch (shown in green in Figure 1) and a NAM-related sub-branch. Besides, the founding member NO APICAL MERISTEM (*PhNAM*, Souer *et al*., 1996)), the NAM sub-branch divides into a dicot group (dark blue in Figure 1) containing CUC2 from *Arabidopsis* (Aida *et al*., 1997) and CUP from *Antirrhinum majus* (Weir *et al*., 2004) and a monocot group (shown in light blue) consisting of the two putative maize paralogues ZmNAM1 or ZmNAM2 together with a single rice protein, OsNAM. PhNAM shares closest homology to members of the dicot and the monocot group and thus occupies a central position in this sub-branch (from now on referred to as the NAM sub-branch). In particular, the NAC domains of AtCUC1, AtCUC2 and AmCUP are 86.7%, 89.8% and 93.4% identical to PhNAM. Although monocots and dicots separated 150 million years ago (Wikström *et al*., 2001), the NAC domain still retains 80.1% and 82.1% identity between PhNAM and ZmNAM1 or ZmNAM2, respectively. Amino acid identity between the ZmNAM1 and ZmNAM2 paralogues is 92.8% in the NAC domain, and they share 89% identity to the rice relative, whereas identity between the maize paralogues declines to 78% over the entire protein-coding region.

In contrast to duplicated *ZmNAM* loci, the NAC domain encoded by a single *ZmCUC3* gene was identified as grouping together with that of a single rice *OsCUC3* representative in a unique sub-branch with the corresponding region in AtCUC3. This distinct CUC3 sub-branch reflects sequence divergence between AtCUC3 and AtCUC1 or AtCUC2 with only 68.7% and 72.9% identity, respectively, whereas identity between the NAC domains of AtCUC1 and AtCUC2 is still 83.7%. In contrast, NAC domain sequence identity between the *Arabidopsis* and monocot *CUC3* relatives exceeds 77% and increases to 94.6% between maize and rice. An overview of the high degree of sequence conservation within the NAC domains of members of the NAM and CUC3 sub-branches illustrates the alignment in Figure 2A.

The other NAC proteins ZmNAC4, ZmNAC5 and ZmNAC6 group outside the NAM/CUC3 branch. However, all branches contain mono- and dicot members, due to availability of genome sequences mainly from rice and *Arabidopsis*. Notably, a close relative to the endosperm-specific *ZmNAC4* gene (see below) could not be identified in the rice genome even though this distinct branch contains two *Arabidopsis* genes and two additional maize endosperm EST's.

Members of the NAM sub-branch share patchy similarity outside the NAC domain referred to as motifs I–IV in Figure 2B. Motifs I and II became evident in a genome-wide comparison of the *NAC* families between *Arabidopsis* and rice (Ooka *et al*., 2003). Inclusion of the PhNAM-related proteins from rice and maize here added motifs III and IV. Motif II provides a *bona fide miR164* binding site in *AtCUC1* and *AtCUC2* (Laufs *et al*., 2004; Mallory *et al*., 2004a) and is identical in all dicot *PhNAM* relatives on the nucleotide level (see alignment below motif II in Figure 2B). We found that a potential miRNA target site is also present in *ZmNAM1/2* and *OsNAM*. This potential monocot-specific miRNA target site exhibits 3 nucleotide differences relative to dicots (shaded in grey) but is strictly conserved among the rice and maize orthologues. Two nucleotide exchanges at non-silent positions relate to the monocot-specific amino acid exchanges (H/L and S/P) in motif II.

Especially pronounced is the conservation of motif IV at the C-terminus between the rice and maize members. This motif is lacking in the shorter AmCUP protein but is evident in PhNAM and AtCUC2, although conservation is reduced.

ZmNAM1/2 *and* ZmCUC3 *expression is associated with SAM formation*

We investigated whether the phylogenetic predictions are substantiated by gene expression patterns during SAM formation in the maize embryo. Figure 3 gives an overview over the different stages of maize embryogenesis. This classification corresponds to the scheme introduced by Abbe and Stein (1954) and is used in all *in situ* hybridisation experiments described below. Median longitudinal sections through maize embryos from early transition to coleoptilar stage (Figure 4) show that *ZmNAM1* is first transcribed at the adaxial side of the *embryo proper* at the position of the SAM anlage during the early transition stage (Figure 4A). Early *ZmNAM1* gene expression is low and extends from the L1 at least 3 cell layers deep into the *embryo proper* (see close-up in Figure 4A). During the mid-transition stage, *ZmNAM1*

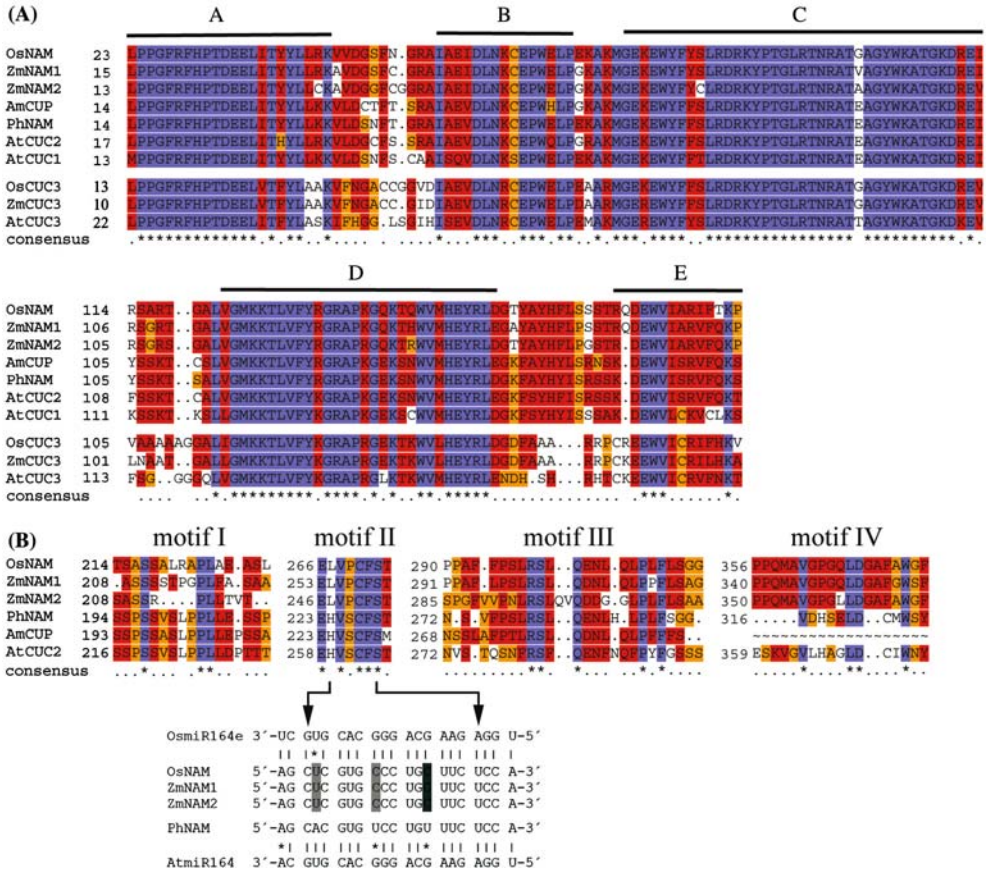

Figure 2. (A) Amino acid comparison of the NAC domain between members of the NAM/CUC3 branch. Conserved sub-domains are indicated by lines (A–E) above the sequences. Note the characteristic deletion between D and E in the CUC3 branch. (B) Conserved protein motifs (I–IV) C-terminal to the NAC domain among members of the NAM sub-branch. The nucleotide sequence of the potential *miR164* target site in the three monocot *NAM* orthologues is compared to the dicot sequence below motif II (*PhNAM* exemplary for dicots). Numbering to the left of each motif indicates the distance to the N-terminus.

transcripts already exhibit a preference for L1 layer of the SAM (Figure 4B) although some expression remains detectable in subtending layers, being particularly pronounced apically, where the coleoptile will emerge (see arrows in the close-up of Figure 4B). The preferential expression in the SAM L1 layer is maintained to the late transition stage, although at the coleoptilar face, *ZmNAM1* expression extends into subtending cell layers (see arrows in Figure 4C). A major change occurs at the coleoptilar stage, where *ZmNAM1* gene expression is downregulated in the centre of the SAM and is confined to a ring-shaped expression domain at the periphery of the SAM. Depicted in Figure 4D and E is a longitudinal and transverse section through a coleoptilar stage embryo. The ring-shaped expression domain is evident in consecutive sections through the SAM (data not shown). The coleoptile emerges outside this ring of *ZmNAM1* expression, which delineates a boundary between SAM and surrounding embryonic tissue. The *ZmNAM2* expression pattern is identical to that of *ZmNAM1* in the coleoptilar stage embryo (data not shown) but the low abundance of *ZmNAM2* transcript did not allow reproducible detection during earlier stages. The pattern or timing of *ZmNAM2* gene expression therefore could exhibit differences compared to *ZmNAM1* during early embryogenesis. However, expression of both *ZmNAM1* and *ZmNAM2* ceases after leaf stage 1.

A different gene expression pattern is detected for *ZmCUC3* (Figure 4F–I). Slightly later than for *ZmNAM1*, initial *ZmCUC3* transcriptional activity is observed during the mid-transition stage in the L1/L2 layers of the SAM anlage (Figure 4G,

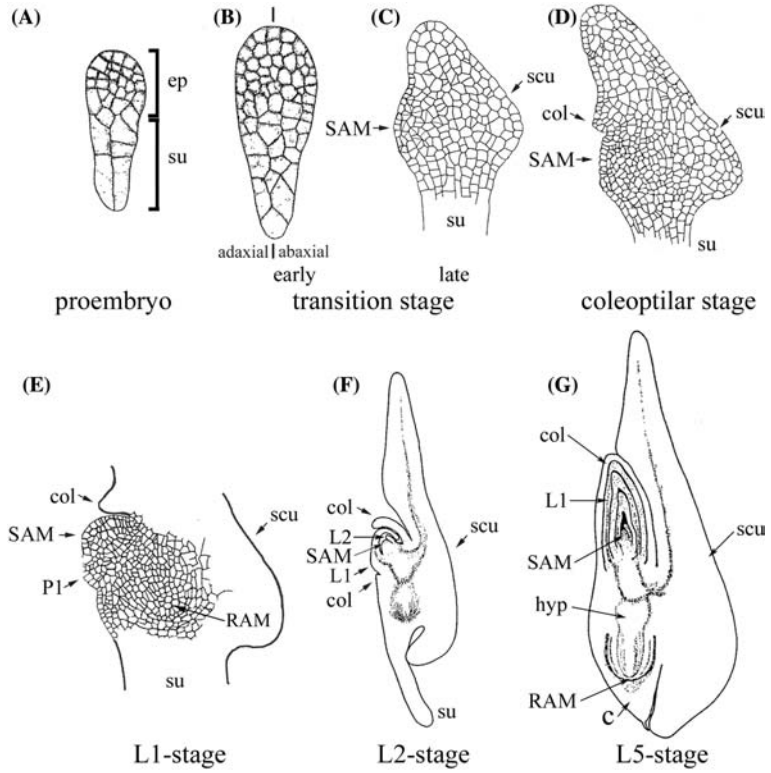

Figure 3. Overview of successive stages of maize embryogenesis (modified after Randolph (1936); classification according to Abbe and Stein (1954). (A) After the first division of the zygote, a series of cell divisions in unpredictable planes gives rise to the small *embryo proper* (ep) and the larger suspensor (su). (B/C) During the transition stage, adaxial/abaxial polarity is manifested by outgrowth of the scutellum (scu) at the abaxial side of the embryo. By the late transition stage, the SAM is evident as a group of cytoplasm-rich cells on the adaxial side. (D) At the coleoptilar stage, the coleoptile becomes evident histologically above the SAM. (E) Activity of the SAM is detected at the leaf stage 1 by emergence of the first leaf primordium (P1) opposite to the coleoptile. Note that the shoot-root axis is oriented in an oblique angle relative to the apical-basal polarity of the proembryo (RAM-root apical meristem). (F) The second leaf (L2) is initiated opposite to the first leaf (L1). (G) In the mature maize embryo, the coleoptile encloses the SAM together with the six leaves initiated in distichous phyllotaxy. The RAM is protected by the coleorhiza (c, hyp: hypocotyl).

compared to F). At the late transition stage, expression is more pronounced and is preferentially detected towards the basal side of the SAM, where the first true leaf (L1) will shortly emerge (marked by an asterisk in Figure 4H). At the coleoptilar stage, *ZmCUC3* transcripts are not detectable in the SAM but persist at the apical boundary to the coleoptile (open triangle in Figure 4I) and are more abundant at the basal face of the SAM towards the L1 leaf (arrows in Figure 4I). In contrast to the ring-shaped activities of *ZmNAM1* or *ZmNAM2*, which cease after the SAM becomes functional, *ZmCUC3* expression persists during later embryo stages. The expression pattern is dynamic, with a clear preference for the boundary/base of the most recent leaf primordium (see below). In conclusion, the expression patterns of *ZmNAM1/2* and *ZmCUC3* in the maize embryo reinforce their association with SAM function as suggested by phylogeny.

ZmNAM1 *and* kn1 *are co-activated in the early maize embryo*

The timing and pattern of early *ZmNAM1* gene expression suggested a close correlation with the gene expression pattern of *knotted1* (*kn1*, Vollbrecht *et al*., 1991; Smith *et al*., 1995). As for *STM* in *Arabidopsis*, *kn1* confers meristematic identity (Kerstetter *et al*., 1997) and is the first marker presently available in maize to monitor formation of the SAM during embryognesis (Smith *et al*., 1995).

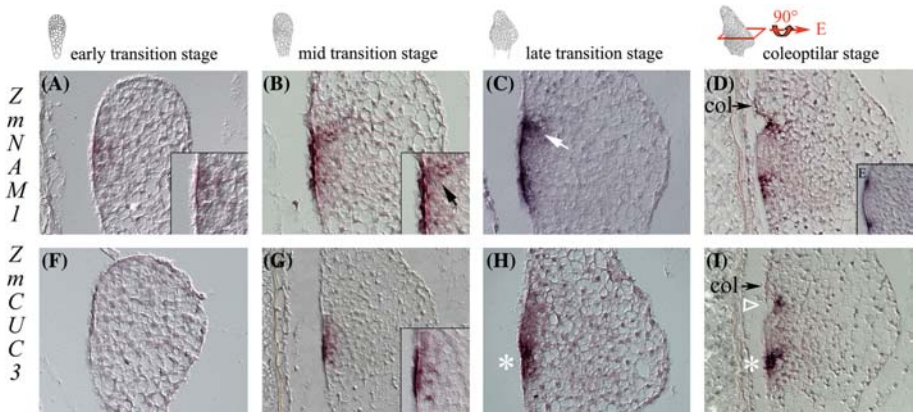

Figure 4. *ZmNAM1* and *ZmCUC3* gene expression in early maize embryos. Successive embryonic stages (from left to right) are schematically indicated above the longitudinal sections. Upper panel (A–D): sections hybridized with the *ZmNAM1* anti-sense probe. Lower panel (F–I): sections hybridized with the *ZmCUC3* probe. The arrow in (C) marks *ZmNAM1* gene expression in deeper layers at the apical flank of the SAM. At the cellular level, *ZmNAM2* transcriptional activity is undetectable prior to the coleoptilar stage, the later pattern is similar to that depicted for *ZmNAM1*. (E) Transverse section as indicated in the drawing above showing *ZmNAM1* expression at the SAM periphery. (F) *ZmCUC3* gene expression is not detected prior to the mid-transition stage (compare to G). Note the preference of *ZmCUC3* gene expression at the basal side of the SAM (indicated by the asterisk in H and I), where the L1 leaf will form. The open triangle in (I) marks transcriptional activity at the apical flank of the SAM towards the coleoptile. The coleoptile emerges outside the ring of *ZmNAM1*/*ZmCUC3* expression.

As shown in Figure 5A and B, *ZmNAM1* and *kn1* transcriptional activity is detected simultaneously at the adaxial face of the transition stage embryo on side-by-side sections. Both expression patterns show significant overlap, although the *kn1* domain extends into deeper layers than the *ZmNAM1* domain. In contrast to previous reports, however, *kn1* transcripts accumulate in the L1 layer during this earliest stage of gene expression (see close-up of Figure 5B for a slightly older embryo). During the mid- to late transition stage, *kn1* transcripts are excluded from the L1 layer of the SAM anlage (see arrow in Figure 5D), whereas *ZmNAM1* gene expression becomes confined to the outermost cell layer (arrow in Figure 5C). Subsequently, at the coleoptilar stage, a ring of *ZmNAM1* expression demarcates a peripheral boundary between the embryonic shoot meristem and external embryonic tissue before the first leaf primordium becomes obvious histologically (Figure 5E). The coleoptile emerges outside this ring-shaped *ZmNAM1* expression domain.

In summary, *ZmNAM1* and *kn1* are activated simultaneously at the adaxial face of the early transition stage embryo. From initially overlapping expression domains a mutually exclusive pattern is acquired by the late transition stage, where *ZmNAM1* mRNA is preferentially found in the L1 layer and *kn1* transcripts are confined to subtending layers of the SAM anlage. At the coleoptilar stage, a ring-shaped *ZmNAM1* expression domain defines the SAM periphery.

ZmCUC3 *gene expression marks lateral organ boundaries throughout plant development*

In contrast to *ZmNAM1* or *ZmNAM2*, *ZmCUC3* remains active in the SAM during later embryonic stages. Median longitudinal sections through leaf-stage I embryos (Figure 6A) show four spots of *ZmCUC3* gene expression, which are located at the boundary between coleoptile and leaf 1 (arrows 1 and 2) and at the boundary between leaf 1 and the SAM (arrows 3 and 4). Corresponding twin spots of expression are expected at each face of the SAM because both the coleoptile and leaf 1 encircle the SAM. The continuous rings of *ZmCUC3* gene expression are more evident in consecutive transverse sections (Figure 6C–E, see schematic drawing in B) and appear as migrating spots (1*/2* and 3*/4*) due to the oblique angle between the shoot axis and the apical/basal polarity of the maize embryo.

ZmCUC3 transcriptional activity at the boundary between the SAM and lateral organ primordia is observed throughout maize development. The

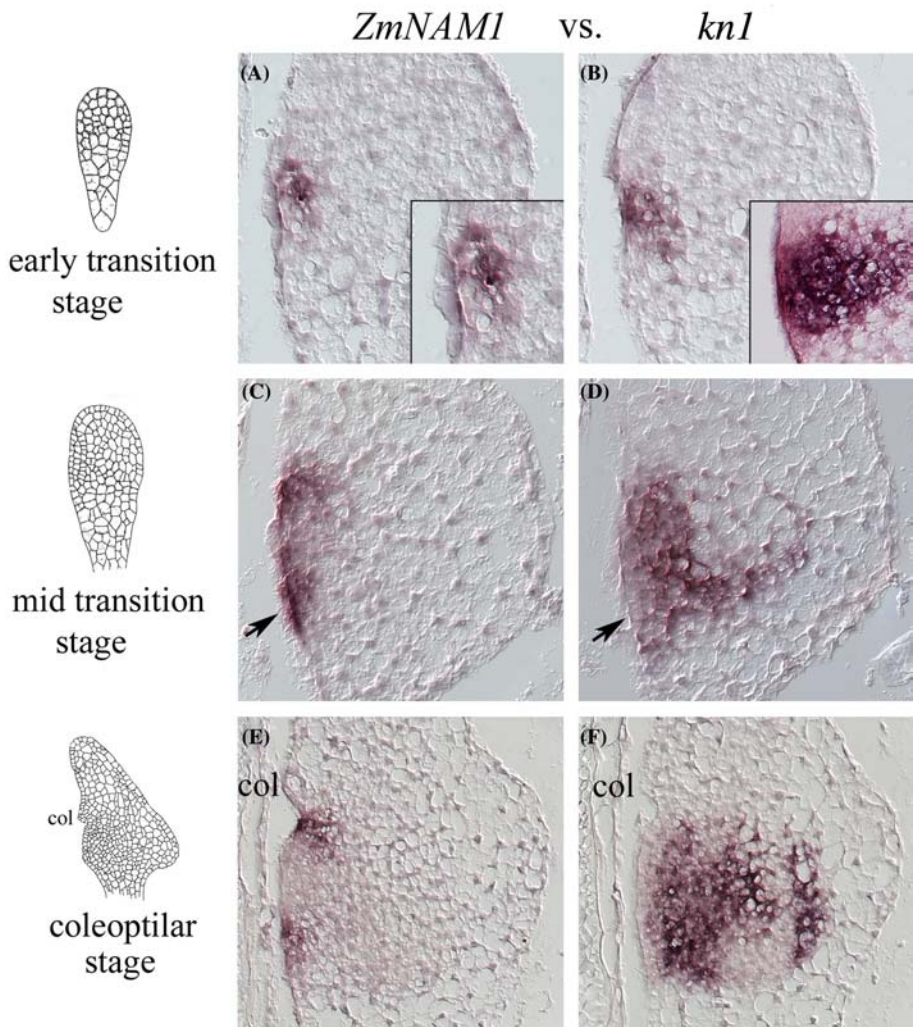

Figure 5. Dynamics of the *ZmNAM1* gene expression pattern relative to that of *kn1* on side-by-side sections. The sections depicted in A, C and E was hybridized with the *ZmNAM1* probe, the adjacent sections B, D and F show hybridisation with the *kn1* probe. Starting form an overlapping pattern (A and B), gene expression domains separate during the mid-transition stage (C and D, arrows indicate the presence of *ZmNAM1* gene expression in the adaxial L1-layer in C and lack of *kn1* transcripts in D) until *ZmNAM1* expression is confined to a ring-shaped domain encircling the SAM (compare E and F; col: coleoptile).

transverse section through the vegetative seedling SAM (Figure 6F) shows a sickle-shaped domain of *ZmCUC3* expression at the base of the P1 primordium, indicating which fraction of the apex has been recruited into the new primordium. This *ZmCUC3* expression domain is U-shaped and extends from the SAM apex into the emerging primordium (Figure 6F). *ZmCUC3* gene expression is also found at the boundary between subtending leaves (P2 depicted in Figure 6G) thus delineating boundaries between individual phytomers at an early stage. A similar expression pattern is observed for *ZmNAM1* in the adaxial epidermis, however, in contrast to the *ZmCUC3* expression pattern, *ZmNAM1* gene expression does not extend beyond the base of the primordium (Figure 6H). *ZmNAM1* transcripts therefore are confined to the primordial side. Neither RNA *in situ* hybridisations nor RT-PCR experiments detected any *ZmNAM2* expression during the vegetative phase (data not shown).

Transcriptional activity of all three genes is again detected in the male and female inflorescence. The *ZmCUC3* gene expression pattern

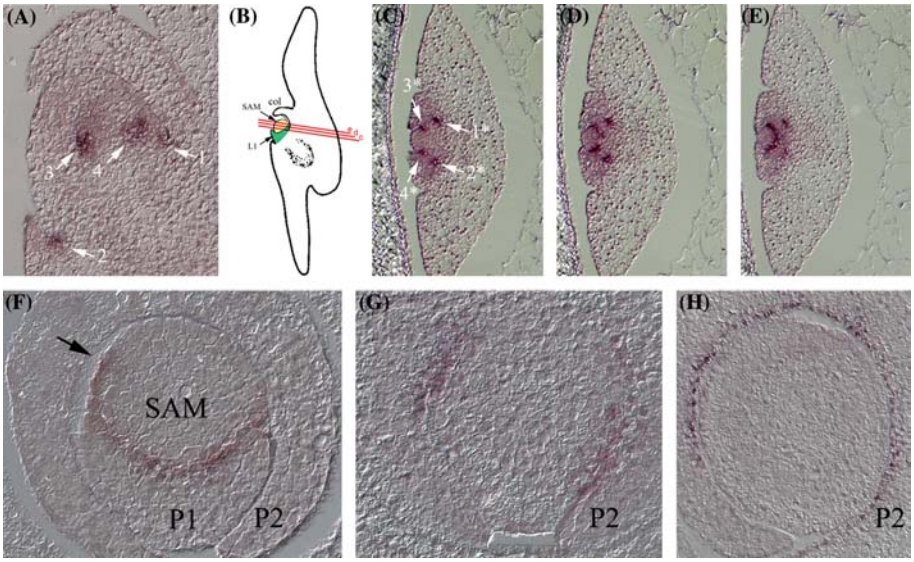

Figure 6. *ZmCUC3* expression during vegetative development. (A) Longitudinal section through a leaf stage 1 embryo. Arrows 1 and 2 indicate *ZmCUC3* gene expression between the coleoptile and the abaxial side of leaf 1. Arrows 3 and 4 correspond to *ZmCUC3* gene expression detected at the boundary between the adaxial side of L1 and the SAM. (B) Schematic drawing indicating the position of transverse sections depicted in C, D and E. Arrows 1* and 2* in C indicate the boundary between coleoptile and L1 leaf 1, arrows 3* and 4* the boundary between L1 and the SAM. Note continuity of the expression domain between the SAM and the L1 leaf in E. (F) Transverse section through the seedling SAM at the base of the P1 primordium, indicating which area of the apex is committed to the arising P1 primordium. The arrow indicates expression in cells of the SAM. (G) *ZmCUC3* transcriptional activity at the boundary between P1 and P2. (H) *ZmNAM1* expression in the adaxial epidermis of the P2 leaf.

remains restricted to boundaries between the spikelet pair meristem (SPM), spikelet meristem (SM) or floral meristem (FM). In contrast, *ZmNAM1* and weaker *ZmNAM2* gene expression is initially associated with meristem anlage. Adjacent sections through the SM (Figure 7A and B) show this pronounced difference, with the apical dome of the SM devoid of *ZmCUC3* transcript, but showing strong *ZmNAM1* expression. According to consecutive sections, both genes are co-transcribed in a ring-shaped expression domain at the SM base (data not shown). The boundary-specificity of *ZmCUC3* gene expression is especially evident in the stage E ear spiklet (floral stages according to Cheng *et al*., 1983). Transcriptional activity marks the boundary between the upper floral meristem and inner/outer lemma and is also detected at the base of the glumes (Figure 7C), whereas the adjacent section hybridized with the *ZmNAM1* probe shows gene expression in the upper floral meristem (Figure 7D). Similar to the seedling SAM, *ZmCUC3* expression therefore separates lateral organs and precedes histological appearance of new primordia in the flower.

Residual ZmNAC *genes also exibit high cell-type specificity*

The ZmNAC4-6 proteins cluster outside the NAM/CUC phylogenetic branch. *ZmNAC4* is expressed in the developing endosperm beginning with the onset of cellularisation (about 6 days after pollination (dap) data not shown). The close-up in Figure 8A illustrates the absense of *ZmNAC4* transcripts in the aleurone layer. These so-called subaleurone cells originate by periclinal divisions of aleurone cells and redifferentiate to become starchy endosperm cells. *ZmNAC4* transcription thus provides an early and selective marker for the acquisition of endosperm cell fate. In the embryo, *ZmNAC4* gene expression is detected only transiently in a few cells of the provascular system in leaf-stage I embryos (data not shown). However, we cannot exclude cross-hybridisation with transcripts corresponding to the closely related ESTs ZmCD44437084 or Zm443430 (see Figure 1).

ZmNAC5 and *ZmNAC6*, putative paralogues, exhibit highly similar embryonic expression patterns. During embryogenesis, both gene transcripts are confined to the coleorhiza. Embryonic

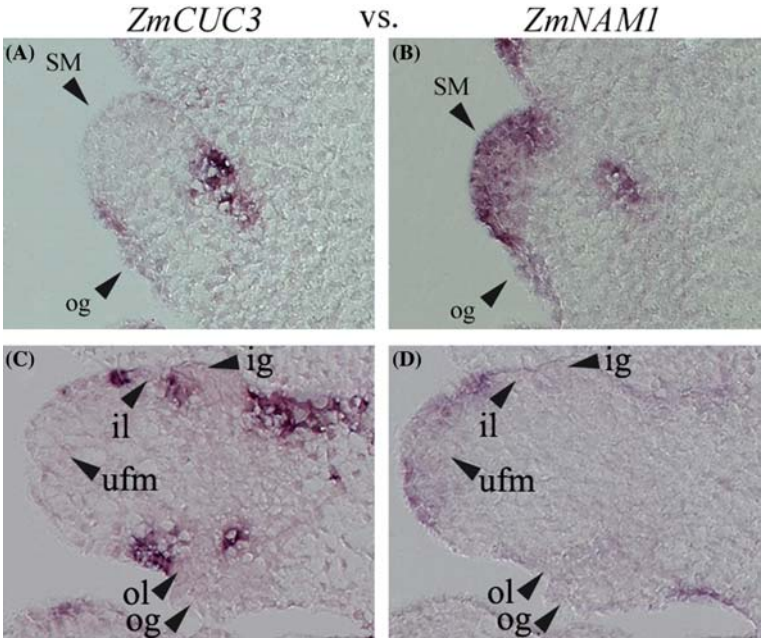

Figure 7. *ZmCUC3* and *ZmNAM1* expression in the female inflorescence compared in side-by-side sections. A and B: Spikelet meristem with *ZmCUC3* expression at the base (A) and *ZmNAM1* expression in apex and at the base (B). C and D: Stage E flower *ZmCUC3* expression (C) is detected at the base of the flower, outer glumes (og), outer lemma (ol), inner glume (ig), inner lemma (il) and the boundary to the upper floral meristem (ufm). In contrast, *ZmNAM1* expression (D) in the neighbouring section is detected in the upper floral meristem.

ZmNAC5 expression is specific to the coleorhiza (see Figure 8B for a leaf-stage 3 embryo and Figure 8C for a mature embryo), whereas *ZmNAC6* transcription, which is activated slightly earlier than that of *ZmNAC5* during the mid-transition stage, is transiently detected in the vasculature of leaf stage 3–4 maize embryos (data not shown). In contrast to *ZmNAC6* expression, *ZmNAC5* transcriptional activity is detected in the root cap of the primary root during the vegetative phase (Figure 8D). This *ZmNAC5* expression domain is comprised of 4–5 cell-layers subtending the quiescent center (QC) of the root apical meristem (RAM) and includes the calyptrogen, the root cap meristem layer. The shared cellular identity in coleorhiza and root cap suggested a comparison between the *ZmNAC5/6* expression pattern and that of *ZmSCR*, an endodermis/QC specific marker (Lim *et al.*, 2000). Consecutive sections showed that *ZmNAC6* is active at the mid-transition stage in a central domain below that of the cup-shaped *ZmSCR* domain (compare Figure 8E and F). *ZmNAC6* thus displays apical/basal patterning of the maize root already at this early stage of embryogenesis.

Discussion

NAM/CUC3 *phylogeny*

NAC domain phylogeny distinguishes two discrete gene sub-branches: A larger *NAM* sub-branch, which is comprised of *PhNAM*, *AmCUP*, *AtCUC1*, *AtCUC2* together with *OsNAM* and the *ZmNAM1/ZmNAM2* maize paralogues, and a second smaller *CUC3* sub-branch containing *AtCUC3*, *OsCUC3* together with a single *ZmCUC3* maize orthologue. Monocot and dicot members in each sub-branch suggest that distinct *NAM* and *CUC3* gene functions presumably existed before mono- and dicot species separated. *PhNAM* occupies a central position in the *NAM* sub-branch as even amino acid identity to the monocot members exceeds 80%. *PhNAM* groups together with *AtCUC2*, whereas *AtCUC1* is rooted outside the main bough. An *AtCUC1* orthologue could still exist in the maize genome, but therefore might also be expected to be present in the fully sequenced rice genome (Goff *et al.*, 2002). Its absence in rice suggests that *AtCUC1* might represent gene duplication peculiar to *Arabidopsis*, whereas a common

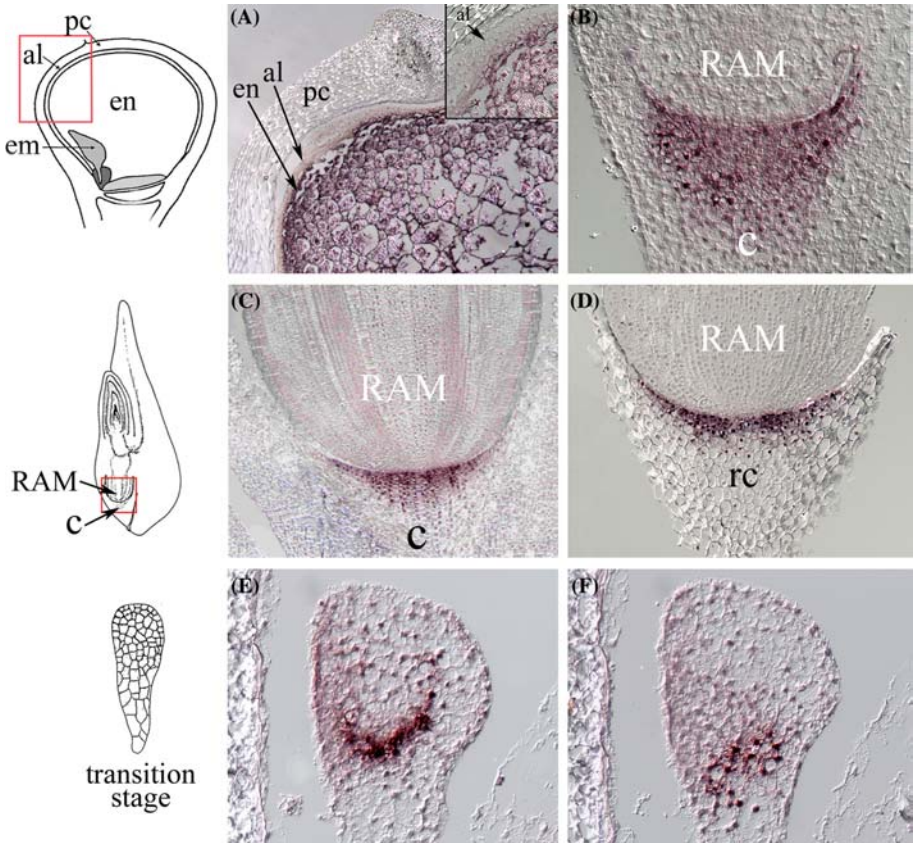

Figure 8. (A) Expression of *ZmNAC4* in the endosperm (en); the outer aleurone cell layer (al) is free of transcripts (see close-up; em: embryo, pc: pericarp). (B–D): *ZmNAC5* gene expression detected in the coleorhiza of a leaf stage 1 embryo (B), at the leaf stage 3 (C) and in the root cap of the germinating seedling (D). (E) and (F): adjacent sections through a mid-transition stage embryo: (E) The *ZmNAC6* gene expression domain is located below the cup-shaped *ZmSCR* domain (shown in F), which at its base marks the position of the prospective quiescent centre.

ancestor of mono- and dicot species might have contained only single *NAM*- and *CUC3*-type precursors.

The difference between members of the *NAM* and *CUC3* sub-branches gains support by sequence conservation downstream of the NAC domain. Only of *NAM* sub-branch members exhibit conservation of 4 motifs (I-IV, see Fig. 2B). Motif II contains a target site of micro RNA *miR164*, which is strictly conserved between *AtCUC1, AtCUC2*, *AmCUP* and *PhNAM*. This level of post-transcriptional control has been shown for *AtCUC1* and *AtCUC2* (Mallory *et al*., 2004a; Laufs *et al*., 2004), and the strict target site conservation suggests that it may be ancient in the *NAM* sub-branch. This potential target site is conserved in monocot *NAM*-type genes. However, it is absent in the *CUC3* sub-branch supporting an early separation of *PhNAM* and *AtCUC3* functions. The putative monocot recognition site is identical in *ZmNAM1*, *ZmNAM2* and *OsNAM* but exhibits three nucleotide differences in comparison to its dicot counterpart (*miR164* position 8, 13 and 21). Interestingly, two U/C transitions (position 8 and 13) in *ZmNAM1/2* or *OsNAM* compensate mismatches between *AtmiR164* and the dicot target site, whereas an A/U transversion (position 21) introduces a new mismatch (see Figure 2B). On the protein level motif II exhibits two characteristic amino acid exchanges (L/H and P/S) between mono- and dicot *NAM* orthologues. Degeneracy of the genetic code would allow multiple sequence permutations without affecting the protein sequence, however, nucleotides are exchanged at two non-silent positions (*miR164* position 13 and 18). Thus, differences in the

sequence of the potential monocot miRNA target site could either reflect compensatory changes to the corresponding miRNA or functional constraints exerted at the protein level.

In conclusion, the presence of a potential miRNA target site in members of the *NAM* sub-branch and its absence in the *CUC3* sub-branch supports the discrete phylogenetic classification based on the NAC domain. Ancestral *NAM*- and *CUC3*-type genes therefore presumably existed prior to the separation of monocot and dicot lineages.

Cellular expression patterns

The sequence-based phylogeny is considerably substantiated by the cellular expression patterns of *ZmNAM1/2* and *ZmCUC3*. A major difference is that *ZmCUC3* gene expression is restricted to the boundary between the SAM and lateral organ primordial whereas in an early pattern *ZmNAM1/2* transcription is always associated with the anlagen of meristems. This is most evident in the early transition stage embryo, where *ZmNAM1* is co-activated in an overlapping gene expression pattern with *kn1*. The initial coincidence of *ZmNAM1/2* transcriptional activity with that of the meristem identity marker *kn1* suggests that one *ZmNAM1/2* function may be in the establishment of meristems. This assumption is consistent with the phylogeny since both maize paralogues group in one sub-branch with PhNAM and AtCUC2 which essentially contribute to the anlage of the SAM in *Petunia* or *Arabidopsis*, respectively (Souer *et al*., 1996; Aida *et al*., 1997). Subsequently, the *ZmNAM1/2* expression patterns acquire complementarity to the *kn1* domain similar to the mutually exclusive patterns of *AtCUC2* and *STM* in *Arabidopsis* (Aida *et al*., 1999) until ultimately a ring of *ZmNAM1/2* and *ZmCUC3* gene expression encircles the SAM at its periphery. The dynamics of the *ZmNAM1* and *ZmCUC3* expression patterns relative to that of *kn1* are depicted in the schematic drawing shown in Figure 9. This *ZmNAM1/2* gene expression pattern may in part be controlled post-transcriptionally. Whereas, the early *ZmNAM1/2* transcription pattern may only depend on promoter activity, its confinement to the outermost L1 layer or the SAM periphery at later stages could be under *miR164* control. This is suggested by experimental results in *Arabidopsis*, where expression of a *miR164*-resistant form of the *AtCUC2* mRNA in the periphery of the SAM causes severe leaf defects (Laufs *et al*., 2004). The degradation of *AtCUC2* transcripts at the outer periphery of the SAM therefore appears essential to establish proper primordial cell identity in *Arabidopsis*.

In the maize embryo, *ZmCUC3* transcriptional activity is detected later than that of *ZmNAM1/2*. This timing is clearly different to in *Arabidopsis*, where *AtCUC3* is already activated in the octant stage embryo significantly earlier than *AtCUC1* or *AtCUC2* (Vroemen *et al*., 2003). However, patterning of the maize and *Arabidopsis* embryo shows significant differences. Whereas, the SAM is initiated at an apical position of the *Arabidopsis* embryo (Long and Barton, 1998), it is established at an adaxial lateral position in the maize embryo (Bommert and Werr, 2001). In the globular *Arabidopsis* embryo, expression of all three genes *AtCUC1*, *AtCUC2* and *AtCUC3* precedes the activation of meristem identity genes, such as *STM*, which is considered orthologous to *kn1* in maize. Moreover, *AtCUC* functions are necessary to activate *STM* in a stripe-shaped pattern during the late globular stage and only assume a pattern complementary to that of *STM* during the heart stage of *Arabidopsis* embryogeny. The SAM anlage is thus delineated centrally within a stripe of *AtCUC* gene expression, which essentially contributes to the full separation of two cotyledons and to the earlier acquisition of bilateral symmetry in the dicot embryo (Aida *et al*., 1999). In contrast, the formation of the scutellum at the abaxial face of the *embryo proper* and the SAM towards its opposite adaxial face comprise adaxial/abaxial polarity in the monocot embryo. The lack of bilateral symmetry in the monocot embryo thus coincides with an absence of *ZmNAM1*, *ZmNAM2* and *ZmCUC3* gene expression before cells are recruited for the SAM anlage. Similar to in *Arabidopsis*, however, *ZmNAM1* and *ZmNAM2* gene expression is detected in cells of the prospective SAM together with *kn1*. A major difference in maize compared to *Arabidopsis* is the absence of early *ZmNAM/ZmCUC3* gene expression whereas, all three *AtCUC* genes prepattern the first plane of bilateral symmetry in the dicot embryo (Aida *et al*., 1999; Vroemen *et al*., 2003).

Maize, as a typical representative of grasses, exemplifies the most complex embryo development in plants. The coleoptile is an organ without

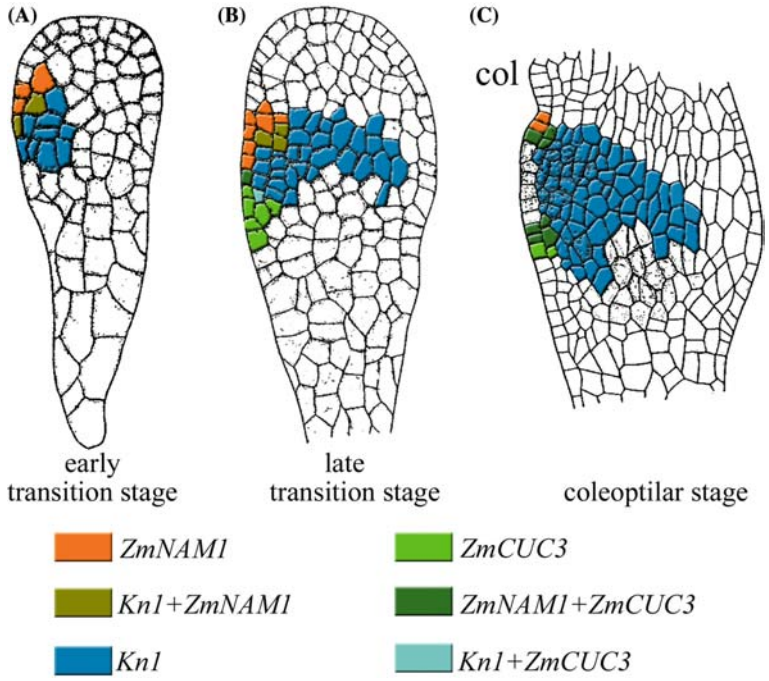

Figure 9. Schematic representation of SAM establishment in the maize embryo between early transition and late coleoptilar stage. The colour code indicates individual or combinatorial activities of *kn1*, *ZmNAM1* and *ZmCUC3*.

counterpart in dicot species and protects the embryonic shoot plumule during germination. The discussion about its origin is controversial, but histologically, the coleoptile becomes evident outside of the ring of *ZmNAM1/2* or *ZmCUC3* gene expression which delineates a precise boundary between the SAM and surrounding embryonic, mostly scutellum tissue. This observation substantiates the *Kn1* loss-of function phenotype in specific inbred backgrounds, where the coleoptile develops in the absence of a functional SAM (Vollbrecht *et al*., 2000) or in the absence of the coleoptile, although the SAM achieves transcriptional activity (Elster *et al*., 2000). Coleoptilar cells are recruited from extra-SAM tissue in a manner clearly different to the initiation of leaf primordia from the SAM. Leaf cell recruitment is best seen in transverse sections through the seedling plumule, where the *ZmCUC3* gene expression pattern at the base of the P1 primordium indicates that about 1/3 of the SAM area is committed for recruitment. At the position of the midrib, the *ZmCUC3* expression boundary extends 7–8 cell layers deep into the SAM, consistent with sectorial data showing that cells central to the apex may contribute to successive phytomers at both faces of the stem axis (Bossinger *et al*., 1992). *ZmCUC3* gene expression is also found later also at the boundary between elaborated phytomers P1 and P2, and more weakly between earlier phytomers. In embryo, seedling and flower, *ZmCUC3* gene expression delineates the boundary between existing or prospective lateral organs, which is also considered to be the main contribution of *AtCUC3* in *Arabidopsis* (Vroemen *et al*., 2003).

Cell identities are shared between coleorhiza and root cap

Transcriptional activity of *ZmNAC5* and *ZmNAC6*, putative paralogues, is highly specific to the coleorhiza, which is an embryonic organ unique to the family of *Poaceae* (Tillich, 1977) and protects the primary root during germination. In *Arabidopsis*, the root is specified at the boundary between the *embryo proper* and the single uppermost cell of the suspensor, the hypophysis (Jürgens, 1992). At the mid-transition stage maize embryos show *ZmNAC6* gene expression centrally overlapping with the cup-shaped *ZmSCR* expression domain, which marks the endodermis throughout the quiescent centre (Lim *et al*.,

2000). *ZmNAC5* gene expression is activated only slightly later. The *ZmNAC5/6* expression domain extends well below that of *ZmSCR* and these expression patterns subsequently become mutually exclusive, with the *ZmNAC5/6* expression domain becoming confined to the coleorhiza. In the mature embryo, *ZmNAC5/6* gene expression is confined to the basal coleorhiza region comprising a continuous cell array with the root apical meristem (RAM), whereas the coleorhiza detaches laterally from the primary root. This expression domain at the basal tip of the embryonic coleorhiza is very similar to that of *ZmNAC5* in the seedling root cap (*ZmNAC6* is inactive in the seedling) where transcripts are detected in 4–5 cell-layers subtending the QC including the root cap meristem layer, the calyptrogen. Based on the *ZmNAC5* expression pattern, the tip of the embryonic coleorhiza shares cellular identity with the root cap.

In the *Arabidopsis* embryo, the root cap (columella) is derived from the hypophyseal cell, which gives rise to an upper lens-shaped QC progenitor cell and a lower columella precursor (Aida *et al.*, 2004). The shared cell identity of coleorhiza/root cap and the early *ZmNAC5/6* expression pattern below the *ZmSCR* expression domain in the mid-transition stage embryo suggest that specification of the QC and the progenitor cells of coleorhiza/root cap occurs at a central position internally of the maize embryo. This specification cannot depend on single cell contacts between the hypophysis and the embryo *proper* as in *Arabidopsis* but has to involve radial positional information established within the maize embryo. The RAM anlage within the maize embryo has consequences for later development. Rapid outgrowth of the primary root during germination depends on cell expansion and requires release of the root from enclosing embryonic tissue. Whereas the embryonic cell array is dissolved laterally between cells recruited for root or coleorhiza, it remains continuous at its base, where cellular identity is shared between coleorhiza and root cap. According to the gene expression pattern of the *ZmNAC5* molecular marker the base of the coleorhiza could be considered as primary root cap. Only its lateral detachment from root progenitor cells gives rise to a distinct embryonic cell fate outside the root. On the protein level, *ZmNAC5* and *ZmNAC6* share high sequence identity with the *OsNAC7* gene, which is expressed in rice embryos (Kikuchi *et al.*, 2000). It will be informative to see whether *OSNAC7* expression possibly supports the shared cell identities between coleorhiza and root cap in a second *Poaceae* species.

In summary, we have isolated maize orthologues to the *PhNAM* and *AtCUC* genes in *Petunia* and *Arabidopsis*, respectively. Our phylogenetic analysis indicates the existence of two distinct *NAM* and *CUC3* precursors, which already existed prior to the separation of mono- and dicot species.

The common branch of the two maize paralogues *ZmNAM1* and *ZmNAM2* together with *PhNAM*, *AtCUC2* or *AmCUP* and their expression patterns support their contribution to SAM establishment. In contrast, the *ZmCUC3* orthologue is associated with boundary specification at the SAM periphery where it visualizes which fraction of SAM cells is committed to a new leaf primordium. Other maize *NAC* gene family members clearly locate outside of this *NAM/CUC3* branch but also exhibit highly cell type-specific expression patterns.

Acknowledgements

We thank Dr. Casper Vroemen (Wageningen) for providing the *AtCUC3* protein sequence prior to publication and Dr. Peter Rogowsky for providing the leaf-stage 1 embryo cDNA library used to screen for maize *NAM/CUC* orthologues. We also thank Drs. J. Nardmann and J. Chandler for suggestions, stimulating discussions and critically reading the manuscript. The maize work was supported by the European Commission through QLK3-2000-00196 and QLRT-2000-00302.

References

Abbe, E.C., Phinney, B.O. and Baer, D.F. 1951. The growth of the shoot apex in maize: internal features. Am. J. Bot. 38: 744–752.

Abbe, E.C. and Stein, O.L. 1954. The growth of the shoot apex in maize: embryogeny. Am. J. Bot. 41: 285–293.

Aida, M., Ishida, T. and Tasaka, M. 1999. Shoot apical meristem and cotyledon formation during *Arabidopsis* embryogenesis: interaction among the *CUP-SHAPED COTYLEDON* and *SHOOT MERISTEMLESS* genes. Development 126: 1563–1570.

Aida, M., Ishida, T., Fukaki, H., Fujisawa, H. and Tasaka, M. 1997. Genes involved in organ separation in *Arabidopsis*: an analysis of the cup-shaped cotyledon mutant. Plant Cell 9: 841–857.

Aida, M., Beis, D., Heidstra, R., Willemsen, V., Blilou, I., Galinha, C., Nussaume, L., Noh, Y.S., Amasino, R. and Scheres, B. 2004. The *PLETHORA* genes mediate patterning of the *Arabidopsis* root stem cell niche. Cell 119: 109–120.

Bommert, P. and Werr, W. 2001. Gene expression patterns in the maize caryopsis: clues to decisions in embryo and endosperm development. Gene 271: 131–142.

Bossinger, G., Maddaloni, M., Motto, M. and Salamini, F. 1992. Formation and cell lineage patterns of the shoot apex of maize. Plant J. 2: 311–320.

Bradley, D., Carpenter, R., Sommer, H., Hartley, N. and Coen, E. 1993. Complementary floral homeotic phenotypes result from opposite orientations of a transposon at the plena locus of Antirrhinum. Cell 72: 85–95.

Cheng, P.C., Greyson, R.I. and Walden, D.B. 1983. Organ initiation and the development of unisexual flowers in the tassel and ear of *Zea mays*. Am. J. Bot. 70: 450–462.

Duval, M., Hsieh, T.F., Kim, S.Y. and Thomas, T.L. 2002. Molecular characterization of AtNAM: a member of the *Arabidopsis NAC* domain superfamily. Plant Mol. Biol. 50: 237–248.

Elster, R., Bommert, P., Sheridan, W.F. and Werr, W. 2000. Analysis of four embryo-specific mutants in *Zea mays* reveals that incomplete radial organization of the proembryo interferes with subsequent development. Dev. Genes Evol. 210: 300–310.

Ernst, H.A., Olsen, A.N., Larsen, S. and Lo Leggio, L. 2004. Structure of the conserved domain of *ANAC*, a member of the *NAC* family of transcription factors. EMBO Rep. 5: 297–303.

Goff, S.A. *et al*. 2002. A draft sequence of the rice genome (*Oryza sativa* L. ssp. *japonica*). Science 296: 92–100.

Jackson, D.P. (1991). In situ hybridisation in plants. In: Molecular Plant Pathology: A Practical Approach, Oxford, UK: Oxford University Press.

Jürgens, G. 1992. Pattern formation in the flowering plant embryo. Curr. Opin. Genet. Dev. 2: 567–570.

Kerstetter, R.A. and Hake, S. 1997. Shoot meristem formation in vegetative development. Plant Cell 9: 1001–1010.

Kerstetter, R.A., Laudencia-Chingcuanco, D., Smith, L.G. and Hake, S. 1997. Loss-of-function mutations in the maize homeobox gene, knotted1, are defective in shoot meristem maintenance. Development 124: 3045–3054.

Kikuchi, K., Ueguchi-Tanaka, M., Yoshida, K.T., Nagato, Y., Matsusoka, M. and Hirano, H.Y. 2000. Molecular analysis of the *NAC* gene family in rice. Mol. Gen. Genet. 262: 1047–1051.

Kumar, S., Tamura, K., Jakobsen, I.B. and Nei, M. 2001. MEGA2: molecular evolutionary genetics analysis software. Bioinformatics 17: 1244–1245.

Laufs, P., Peaucelle, A., Morin, H. and Traas, J. 2004. MicroRNA regulation of the CUC genes is required for boundary size control in *Arabidopsis* meristems. Development 131: 4311–4322.

Lim, J., Helariutta, Y., Specht, C., Jung, J., Sims, L., Bruce, W.B., Diehn, S. and Benfey, P. 2000. Molecular analysis of the *SCARECROW* gene in maize reveals a common basis for radial patterning in diverse meristems. Plant Cell 12: 1307–1318.

Long, J.A. and Barton, M.K. 1998. The development of apical embryonic pattern in *Arabidopsis*. Development 125: 3027–3035.

Mallory, A.C., Dugas, D.V., Bartel, D.P. and Bartel, B. 2004a. MicroRNA regulation of *NAC*-domain targets is required for proper formation and separation of adjacent embryonic, vegetative, and floral organs. Curr. Biol. 14: 1035–1046.

Ooka, H., Satoh, K., Doi, K., Nagata, T., Otomo, Y., Murakami, K., Matsubara, K., Osato, N., Kawai, J., Carninci, P., Hayashizaki, Y., Suzuki, K., Kojima, K., Takahara, Y., Yamamoto, K. and Kikuchi, S. 2003. Comprehensive analysis of *NAC* family genes in Oryza sativa and *Arabidopsis* thaliana. DNA Res. 10: 239–247.

Randolph, L.F. 1936. Developmental morphology of the caryopsis in maize. J. Agric. Res. 53: 881–916.

Roth, I. 1955. Zur morphologischen Deutung des Grasembryos und verwandter Embryotypen. Flora 144: 163–212.

Sablowski, R.W. and Meyerowitz, E.M. 1998. A homolog of *NO APICAL MERISTEM* is an immediate target of the floral homeotic genes *APETALA3*/*PISTILLATA*. Cell 92: 93–103.

Smith, G.L., Jackson, D. and Hake, S. 1995. Expression of *knotted1* marks shoot meristem formation during maize embryogenesis. Dev. Genet. 16: 344–348.

Souer, E., vanHouwelingen, A., Kloos, D., Mol, J. and Koes, R. 1996. The no apical meristem gene of Petunia is required for pattern formation in embryos and flowers and is expressed at meristem and primordia boundaries. Cell 85: 159–170.

Steffensen, D.M. 1968. A reconstruction of cell development in the shoot apex of maize. Am. J. Bot. 55: 354–369.

Sussex, I.M. 1989. Developmental programming of the shoot meristem. Cell 56: 225–229.

Tillich, H. 1977. Vergleichend morphologische Untersuchungen zur Identität der Gramineen-Primärwurzel. Flora 166: 415–421.

Vollbrecht, E., Reiser, L. and Hake, S. 2000. Shoot meristem size is dependent on inbred background and presence of the maize homeobox gene, knotted1. Development 127: 3161–3172.

Vollbrecht, E., Veit, B., Sinha, N. and Hake, S. 1991. The developmental gene *Knotted-1* is a member of a maize homeobox gene family. Nature 350: 241–243.

Vroemen, M., Aigner, L., Winkler, J. and Weidner, N. 2003. Adult neural progenitor cell grafts survive after acute spinal cord injury and integrate along axonal pathways. Eur. J. Neurosci. 18: 743–751.

Waites, R. and Simon, R. 2000. Signaling cell fate in plant meristems three clubs on one tousle. Cell 103: 835–838.

Weir, I., Lu, J., Cook, H., Causier, B., Schwarz-Sommer, Z. and Davies, B. 2004. *CUPULIFORMIS* establishes lateral organ boundaries in *Antirrhinum*. Development 131: 915–922.

Wikström, N., Savolainen, V. and Chase, M.W. (2001). Evoltution of the angiosperms: calibrating the family tree. Proc. R. Soc. Lond. B. Biol. Sci. 268 (1482): 2211–2220.

Xie, Q., Frugis, G., Colgan, D. and Chua, N.H. 2000. *Arabidopsis NAC1* transduces auxin signal downstream of *TIR1* to promote lateral root development. Genes Dev. 14: 3024–3036.